

分担研究報告書

コンソミックマウスを用いた DSS/PhIP 大腸発がんの研究

研究分担者 杉江茂幸
金沢医科大学・医学部・腫瘍病理学・特任教授

研究要旨

肥満糖尿病モデル動物であるob/obマウス(OB)及びそのwild typeのC57BL/6Jマウス(WT)に対して、PhIP-DSS炎症性大腸発がんモデルを用い、発がん感受性を比較検討した。WTに比し、OBは、肥満傾向が著明であった。大腸腫瘍は、OB PhIP-DSS群 0/9、OB PhIP群 0/5、OB DSS群 0/4、OB陰性対照群 0/4、WTマウスPhIP-DSS群 4/10(0.70±1.25)、WTマウスPhIP群 0/5、WTマウスDSS群 0/4、WTマウス陰性対照群 0/5であった。これらの結果からWTに比し、OBは、腫瘍発生を認めず、PhIP-DSS炎症性大腸発がんモデルにおける腫瘍発生に抵抗性があると考えられた。体重、肝重量、脂肪量は、WTに比べ、OBで極めて高く、他の臓器重量についても高い傾向を認めた。血清生化学検査では、WTに比べ、OBでは、GOT、GPT、ALP、総コレステロール、LDLが、著高を示し、トリグリセリド値は、高い傾向を認めた。血糖値は逆に低い傾向にあった。細胞増殖マーカーPCNAによる大腸腺管の増殖帯の検討では、WTに比し、OBで低い傾向を認めた。

A. 研究の目的

死亡原因の第1位であるがんの制圧は、国民的課題であり、発がん物質、特に環境中発がん物質のヘテロサイクリックアミンに対する感受性要因の解明は重要である。中でもPhIP、MeIQxは、動物実験において多臓器に発がん性が確認されている。このような環境中発がん物質に対する発がん感受性や抵抗性遺伝子の同定、解析を行うことは発がんの機序、種差、個体差の原因解明に必須であり、得られる成果はがん予防、治療に有用と考えられる。今回、新たに開発したdextran sulfate sodium (DSS) 発癌剤併用短期マウス大腸発がんモデルを用いて、ヘテロサイクリックアミンによる種々の異なる系統のマウスでの発癌感受性の差異を検討し、発癌感受性遺伝子、発癌抵抗性遺伝子の同定のための動物実験を行う。特に、ヘテロサイクリックアミンに関する感受性遺伝子の同定、解明を最終目標とする。

B. 研究の方法

雄ob/obマウス(OB)及びそのwild typeのC57BL/6Jマウス(WT)を各4群に分け、第1群にPhIP 200mg/kg体重胃内強制投与し、1週間後から5日間1.5%DSSを飲水投与し、PhIP投与後4週間後、同処置を再度繰り返した。第2群には、PhIP 2回投与のみ、第3群には、DSS 2回投与のみ、第4群は、無処置群とした。匹数は、OB 1群9匹、

2群5匹、3群4匹、4群4匹。WT 1群10匹、2群5匹、3群4匹、4群5匹とした。実験開始20週間後実験終了し、安楽死、剖検した。剖検時、血清を採取し、中性脂肪、コレステロール、血糖値等を測定した。また、PCNAを染色し、細胞増殖の比較検討を行った。

(倫理面への配慮)

動物実験は、金沢医科大学動物実験指針のガイドラインに準拠して行う。動物愛護の精神に則って動物飼育を行い、動物の処置においては倫理基準を遵守し、安楽死は、深麻酔下、苦痛に配慮する。倫理基準による医学生物学実験法に関する分類におけるカテゴリC(脊椎動物を用いた実験で、動物に対して軽微なストレスあるいは痛み(短時間持続する痛み)を伴う実験)の範囲内の実験である。

C. 研究結果

PHIP+DSS 処置群において、体重は、WT 29.90±0.47に対し、OB 72.95±3.34、肝重量は、WT 1.50±0.12に対し、OB 5.90±0.56と著高を認め、肥満にあった。肝臓は、脂肪肝であった。他の臓器重量についてもOBに高い傾向を認めた。これは、他の処置群でも同じ傾向にあった。大腸に腫瘍は、WTの1群(PhIP+DSS)のみに認められ、OBには発見されなかった。各群の大腸腫瘍の

発生率、平均個数は、WT: PhIP-DSS 群 4/10 (0.70±1.25)、PhIP 群、DSS 群、陰性対照群には腫瘍の発生を見なかった。腫瘍は全て腺腫だった。OB: PhIP-DSS 群、PhIP 群、DSS 群、陰性対照群には腫瘍の発生を見なかった。PhIP+DSS 処置群における細胞増殖マーカーPCNA 染色結果: WT では、1/2~2/3 にあったのに対し、OB において増殖帯が、腺管の底部から全体の 1/3~1/2 と低い傾向にあった。

血清生化学データ: PhIP+DSS 処置群において、血清総コレステロール値: OB 326.2±46.2、WT 106.2±10.9、LDL: OB 84.8±18.8、WT 11.4±2.3、GOT: OB 414.8±171.3、WT 42.6±2.5、GPT: OB 540.8±85.1、WT 27.2±3.8、ALP: OB 1149.6±216.3、WT 305.8±3.6 と OB で著高を示し、トリグリセリド値: OB 151.0±62.4、WT 104.6±23.9 と OB に高い傾向を認めた。血糖値は、OB 282.2±61.5、WT 346.0±40.4 と逆に OB で低い傾向を認めた。他の処置群でも同様傾向を認めた。

D. 考察

以上の結果から OB、WT 間で明らかな感受性の違いが認められた。コンソミックマウスの結果から大腸腫瘍発生と肥満、総コレステロール、トリグリセリド値の関与が示唆されたが、今回の結果は、それと対立するものであり、OB における感受性の低下の要因をさらに探究する必要がある。細胞増殖マーカーの低下は、その 1 因と考えられる。

E. 結論

WT の PhIP-DSS 処置群でのみ腫瘍が発生し、OB での腫瘍発生はなかった。OB での腫瘍発生抵抗性の要因の一つとして、細胞増殖の低下の関与が示唆され、今後、研究を進め、感受性低下の原因を解明しなくてはならない。

F. 健康危険情報

本研究の方法、材料、実験結果、および動物個体が人体の健康に害を及ぼす可能性は全くない。また、危険物、毒物の使用については研究所の危険物、毒物取り扱い規定に準拠した安全な取り扱いを遵守している。

G. 研究発表

1. 論文発表

1. Oyama T, Yasui Y, Sugie S, and Tanaka T: Preclinical assays for identifying natural cancer chemopreventive agents. Scholarly Research Exchange, vol. 2009, Article ID 475963, 2009. doi:10.3814/2009/475963.

2. Oyama T, Yasui Y, Sugie S, Koketsu M, Watanabe K, and Tanaka T: Dietary tricin suppresses inflammation-related colon carcinogenesis in male Crj: CD-1 mice. *Cancer Prev Res.*, 2: 1031-1038, 2009.

2. 学会発表

1. 尾山 武、安井由美子、杉江茂幸、渡邊邦友、田中卓二: Tricin による炎症関連大腸がん抑制効果. 第 25 回日本毒性病理学会、浜松、1 月 27-28 日、2009 年。

2. 杉江茂幸、尾山 武、安井由美子、田中卓二: MeIQx 投与後長期飼育における F344 ラットの心臓病変. 第 25 回日本毒性病理学会、浜松、1 月 27-28 日、2009 年。

3. Takeru Oyama, Yumiko Yasui, Miharuru Kamide, Sotoe Yamamoto, Shigeyuki Sugie, and Takuji Tanaka: A flavone, tricin, suppresses colitis-associated mouse colon carcinogenesis. 9th Korea-Japan Symposium on Cancer and Ageing Research. DamYang Resort, South Korea, March 11-12, 2009.

4. Mihye Kim, Shingo Miyamoto, Yumiko Yasui, Takeru Oyama, Akira Murakami, Shigeyuki Sugie, and Takuji Tanaka: Dietary zerumbone inhibits colon and lung carcinogenesis in mice. 9th Korea-Japan Symposium on Cancer and Ageing Research. DamYang Resort, South Korea, March 11-12, 2009.

5. 尾山 武、安井由美子、杉江茂幸、田中卓二: Tricin による炎症関連大腸がん抑制とその機序の検討. 第 98 回日本病理学会総会、京都、5 月 1-3 日、2009 年。

6. 尾山 武、安井由美子、杉江茂幸、田中卓二、渡邊邦友: Tricin による炎症関連大腸がん抑制とその分子機構の検討. がん予防大会 2009 愛知 (第 16 回日本がん予防学会、第 32 回日本がん疫学研究会、第 10 回日本がん分子疫学研究会)、6 月 16-17 日、2009 年。

7. 尾山 武、安井由美子、杉江茂幸、田中卓二: 炎症関連大腸がんにおけるフラボノイド tricin と高コレステロール血症の影響. 第 24 回発癌病理研究会 8 月 25-27 日 七尾

8. Takuji Tanaka, Yumiko Yasui, Takeru Oyama, and Shigeyuki Sugie: Colorectal cancer chemoprevention by beta-cyclodextrin inclusion compounds of auraptene and 4'-geranyloxyferulic acid. 68th Annual Meeting of the Japanese Cancer Association, October 1-3, 2009.

9. Takeru Oyama, Yumiko Yasui, Shigeyuki Sugie,

Kunitomo Watanabe, and Takuji Tanaka: Dietary flavonoid tricetin suppresses colitis-associated mouse colon carcinogenesis. 68th Annual Meeting of the Japanese Cancer Association, October 1-3, 2009.

10. Shigeyuki Sugie, Takeru Oyama, Yumiko Yasui, and Takuji Tanaka: Effect of BITC and PEITC on BBN-induced urinary bladder carcinogenesis in male F344 rats. 68th Annual Meeting of the Japanese Cancer Association,

October 1-3, 2009.

H. 知的財産権の出願・登録状況

1. 特許取得
(なし)
2. 実用新案登録
(なし)
3. その他
(なし)

分担研究報告書

大腸発がんにおける炎症の関与とその分子機構の解明

研究分担者 中島 淳
横浜市立大学医学部 教授

研究要旨

肥満を背景とした大腸発がんリスク上昇がどのようなメカニズムによるものか、その詳細ははっきりしていない。近年アディポサイトカインなどを含む炎症性・非炎症性サイトカインの関与が報告されてきている。肥満による大腸発がん促進の分子機序として持続的な高インスリン血症が大腸上皮細胞の増殖刺激となり、大腸がん促進に作用していることが主流とされてきた。今回の研究では、既存の報告で明示されてこなかった大腸上皮でのインスリンシグナル活性を調べるとともに、高脂肪食摂取により亢進する大腸上皮増殖および初期発がんに関わる分子機序を調査し、*in vivo* 実験において高脂肪食条件下の大腸上皮で Akt 活性が減弱しており、JNK 活性化が増殖に関与している新しい知見を検証し、JNK 経路が高脂肪食摂取による大腸発がん促進メカニズムのひとつであることを証明した。

A. 研究目的

炎症の分子機序の関与が疑われる肥満関連の大腸発がん促進機序を *in vivo* で検証すること。具体的には、大腸上皮でのインスリンシグナル活性を調べるとともに、高脂肪食摂取により亢進する大腸上皮増殖および初期発がんに関わる分子機序を調査することを目的とした。

B. 研究方法

C57BL/6J マウスを使用し、大腸化学発がん物質アゾキシメタンにより誘導される前がん病変 aberrant crypt foci (ACF) の数を検討し、BrdU labeling index を用いて大腸上皮細胞増殖の活性を評価した。これらを普通食摂取群と高脂肪食摂取群との間で比較検討した。さらに高脂肪食群で大腸上皮細胞の増殖活性が亢進している分子メカニズムを明らかにするため、促進機序に関与の可能性がある様々なタンパクの大腸粘膜における活性状況・発現レベルを検証した。

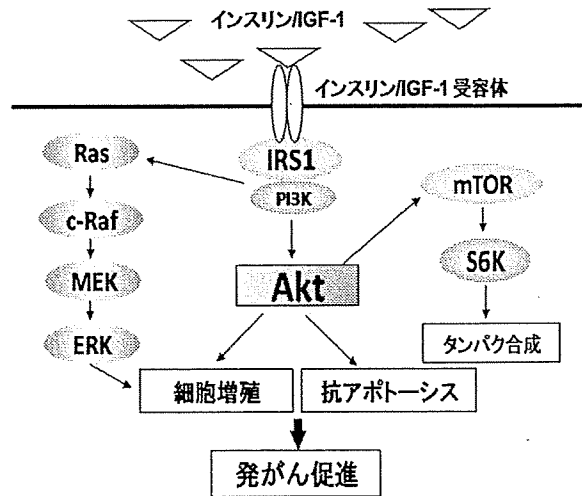
(倫理面への配慮)

当大学の動物実験倫理委員会承認済み。

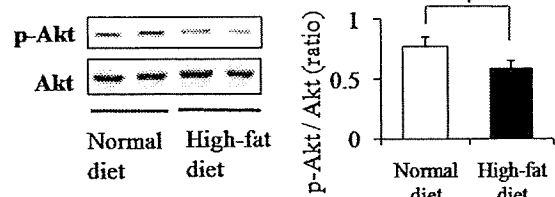
C. 研究結果

ACF の数、BrdU labeling index とともに普通食群と比べ高脂肪食群で有意に増加していた。また血清インスリン値についても普通食群と比較し高脂肪食群で有意に高値であった。これまで高脂肪食

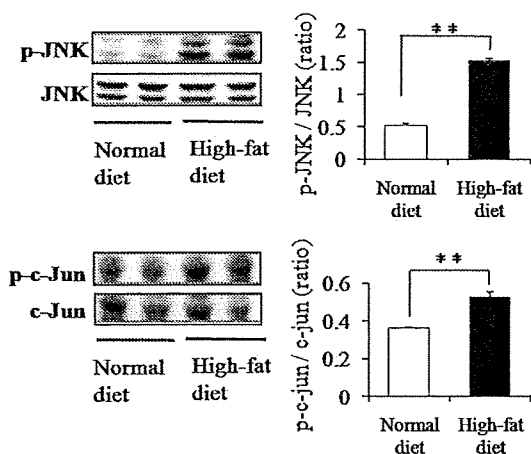
摂取による大腸発がん促進の機序には血清インスリンが高値であることが関与しているとする仮説が有力と考えられてきたため、最初インスリン受容体を介したインスリンシグナル経路が大腸上皮細胞増殖の亢進に関わっていると推測し、まず PI3K/Akt シグナル経路の関与について検討した。



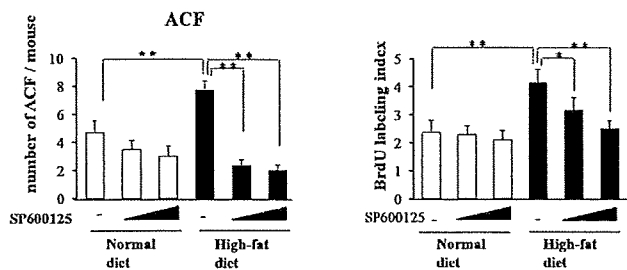
ところが意外なことに、大腸粘膜のウェスタンブロット解析では、普通食群で高脂肪食群より有意に Akt のリン酸化・活性化していた。



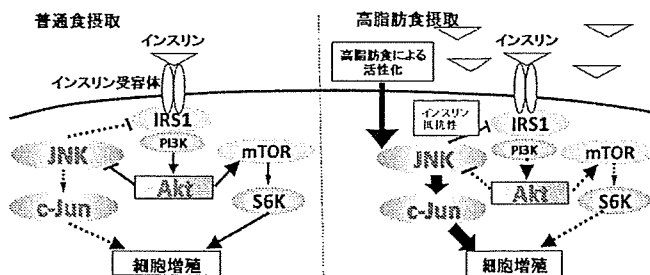
一方で高脂肪食群の IRS-1 のセリンリン酸化は普通食群より有意に亢進しており、Akt リン酸化との間に解離を認めた。IRS-1 のチロシンリン酸化は有意ではないものの高脂肪食群で減弱していた。これらの結果は大腸上皮におけるインスリン抵抗性の存在の可能性を示唆するものであった。IRS-1 のセリンリン酸化はインスリン抵抗性のカギとなるイベントとされており、これまで JNK、ERK、mTOR や S6K など IRS-1 のリン酸化を引き起こす数々のタンパクキナーゼが報告されている。そこで次にこれらのタンパク発現レベルを検証した。リン酸化された ERK、p38MAPK、mTOR や S6K のタンパクレベルは普通食群と高脂肪食群間で違いを認めなかったが、リン酸化 JNK および c-Jun のレベルは高脂肪食群で有意に亢進していた。



JNK/c-Jun シグナル経路は増殖性反応においても非常に重要な構成要素であり、また cyclin D1 は JNK/c-Jun 経路の重要な細胞増殖を引き起こす標的遺伝子とされている。Cyclin D1 のタンパクレベル、mRNA レベルともに高脂肪食群で有意に普通食群よりも高かった。さらに JNK 経路の主要な標的である AP-1 転写因子の活性も高脂肪食群で明らかに増加していた。高脂肪食条件下で JNK 経路が大腸上皮の細胞増殖亢進に直接関与することを確かめるため、ACF 実験において特異的 JNK 阻害薬 SP600125 を使用した。SP600125 投与は、高脂肪食群では用量依存性に ACF 形成と BudU labeling index を有意に抑制したが、普通食群においてはその効果を認めなかった。



さらに JNK 阻害薬は高脂肪食群マウスの大腸のリン酸化 c-Jun タンパクレベル、cyclin D1 タンパクレベルを有意に減弱させた。これらの結果は、高脂肪食摂取条件では JNK 経路の活性化が大腸上皮細胞増殖に重要な働きをしていることを明示する所見である。



D. 考察

従来の報告通り、高脂肪食摂取により大腸上皮細胞増殖は亢進される結果であり、今回はさらにその機序解明に迫った。インスリン受容体を介した PI3K/Akt 経路は増殖亢進に関与しておらず、JNK 活性化が増殖に関与しているという新しい知見を検証し、JNK 経路が高脂肪食摂取による大腸がん促進メカニズムのひとつであることを in vivo で初めて証明した。

E. 結論

肥満関連の大腸がん促進機序のひとつとして JNK 活性化が関与していることが証明された。JNK 上流因子や JNK の正確な役割の究明をさらにすすめる、欧米スタイルの生活習慣の人にとって JNK 経路が予防の標的となりうるかどうかを今後検証が必要である。

F. 健康危険情報

特になし。

G. 研究発表

1. 論文発表

1. Endo H, Hosono K, Fujisawa T, Takahashi H, Sugiyama M, Yoneda K, Nozaki Y, Fujita K, Yoneda M, Inamori M, Wada K, Nakagama H, Nakajima A. Involvement of JNK pathway in the promotion of the early stage of colorectal carcinogenesis under high-fat dietary condition. Gut, 58:1637-43, 2009.

2. Sugiyama M, Takahashi H, Hosono K, Endo H, Kato S, Yoneda K, Nozaki Y, Fujita K, Yoneda M, Wada K, Nakagama H, Nakajima A. Adiponectin inhibits colorectal cancer cell growth through the AMPK/mTOR pathway. Int J Oncol, 34:339-44,

2009.

3. Takahashi H, Takayama T, Yoneda K, Endo H, Iida H, Sugiyama M, Fujita K, Yoneda M, Inamori M, Abe Y, Saito S, Wada K, Nakagama H, Nakajima A. Association of visceral fat accumulation and plasma adiponectin with rectal dysplastic aberrant crypt foci in a clinical population. *Cancer Sci*, 100:29-32, 2009.

4. 内山崇、細野邦広、遠藤宏樹、高橋宏和、中島淳. メタボリックシンドロームと大腸癌. *BIO Clinica メタボリックシンドローム Vol.24 No.4 Apr. 2009*(通巻 309号) 北隆館: 45-51、2009. 4. 10 発行

5. 遠藤宏樹、細野邦広、高橋宏和、中島淳. 高脂肪食制限による大腸発癌抑制の分子機序. *消化器科 Vol.49 No.5 438-443*: 科学評論社. 2009. 11. 28

2. 学会発表

1. 米田恭子、高橋宏和、市川靖史、宇於崎宏、深山正久、油谷浩幸、児玉龍彦、伊藤行夫、相良三奈、宮澤ちひろ、中島淳. 大腸癌の新しい腫瘍マーカーシスタチンSNの開発, 第5回日本消化管学会総会学術集会, 東京, (平成21年1月12日)

2. 細野邦広、遠藤宏樹、加藤真吾、内山崇、飯田洋、馬渡弘典、野崎雄一、秋山智之、米田恭子、藤田浩司、米田正人、高橋宏和、稲森正彦、阿部泰伸、桐越博之、小林規俊、窪田賢輔、斉藤聡、中島淳. メトホルミンによる大腸ポリープ抑制作用の解析—発癌モデルマウスにおける検討—, 第5回日本消化管学会総会学術集会, 東京, (平成21年1月13日)

3. Endo H, Hosono K, Yoneda K, Takahashi H, Nakajima A. JNK plays a crucial role in promotion of the early stage of colon carcinogenesis under the high-fat condition, AACR 100th Annual Meeting 2009, Denver, Colorado, USA (2009. 4. 20)

4. 遠藤宏樹、細野邦広、中島淳. 高脂肪食制限はJNK活性化を抑制して大腸発癌を予防する, 第95回日本消化器病学会, ワークショップ4, 札幌, (平成21年5月)

5. 遠藤宏樹、藤澤聡郎、中島淳. アディポネクチンの大腸発癌に対する効果: 分子メカニズム検討, 第95回日本消化器病学会, シンポジウム5, 札幌, (平成21年5月)

6. 細野邦広、高橋宏和、中島淳. AMPKをターゲットとする新たな大腸化学発癌予防, 第95回日本消化器病学会, ワークショップ4, 札幌, (平成21年5月)

7. 中島淳 第95回日本消化器病学会 一般演題(ポスター) 座長 大腸臨床-3 札幌 (平成21年5月7日)

8. Takahashi H, Hosono K, Endo H, Yoneda K, Akiyama T, Inamori M, Abe Y, Kato S, Uchiyama T, Iida H, Mawatari H, Nozaki Y, Fujita K, Yoneda M, Kobayashi N, Kirikoshi H, Kubota K, Saito S, Nakajima A. Plasma IGF-1 Is Correlated with Dysplastic Aberrant Crypt Foci in Men. *Digestive Disease Week 2009 AGA Institute, Poster Session, Chicago* (2009. 6. 3)

9. 高橋宏和、細野邦広、遠藤宏樹、米田恭子、加藤真吾、内山崇、飯田洋、馬渡弘典、野崎雄一、秋山智之、藤田浩司、米田正人、稲森正彦、阿部泰伸、小林規俊、桐越博之、窪田賢輔、斉藤聡、上野規男、中島淳. Aberrant crypt fociの自然史に対する解析, 第77回日本消化器内視鏡学会総会, 名古屋, (2009年5月21日)

10. 高橋宏和、細野邦広、中島淳. Aberrant crypt fociとサプリメントの相関解析, 第40回日本消化吸収学会総会・第51回日本消化器病学会大会合同, パネスディスカッション24, JDDW, 京都, (平成21年10月17日)

11. 細野邦広、高橋宏和、加藤真吾、内山嵩、鈴木香峰理、飯田洋、馬渡弘典、遠藤宏樹、野崎雄一、坂本康成、米田恭子、藤田浩司、米田正人、阿部泰伸、稲森正彦、小林規俊、桐越博之、窪田賢輔、斉藤聡、中島淳. 生活習慣病からみた大腸癌の新たな化学発癌予防-抗糖尿病薬メトホルミンを用いた検討-, 第51回日本消化器病学会大会, JDDW、京都, (平成21年10月15日)

12. 内山崇、高橋宏和、飯田洋、遠藤宏樹、細野邦広、秋山智之。阿部泰伸、稲森正彦、加藤真吾、渡辺誠太郎、馬渡弘典、米田恭子、野崎雄一、藤田浩司、米田正人、桐越博之、小林規俊、窪田賢輔、斉藤聡、中島淳. 大腸ポリープ、大腸癌の診断に血清レプチン値は有用か, 第51回日本消化器病学会大会, JDDW、京都, (平成21年10月15日)

H. 知的財産権の出願・登録状況 (予定を含む)

1. 特許取得
なし

2. 実用新案登録
なし

3. その他
特になし

研究成果の刊行に関する一覧表レイアウト (参考)

書籍

著者氏名	論文タイトル名	書籍全体の編集者名	書籍名	出版社名	出版地	出版年	ページ
内山崇、 細野邦広、 遠藤宏樹、 高橋宏和、 中島淳	メタボリックシン ドローームと大腸癌	黒川清	BIO Clinica メタボリック シンドローーム	北隆社	日本	2009年	45-51
遠藤宏樹、 細野邦広、 高橋宏和、 中島淳	高脂肪食制限によ る大腸発癌抑制の 分子機序	佐藤信紘	消化器科	科学評論 社	日本	2009年	438-443

雑誌

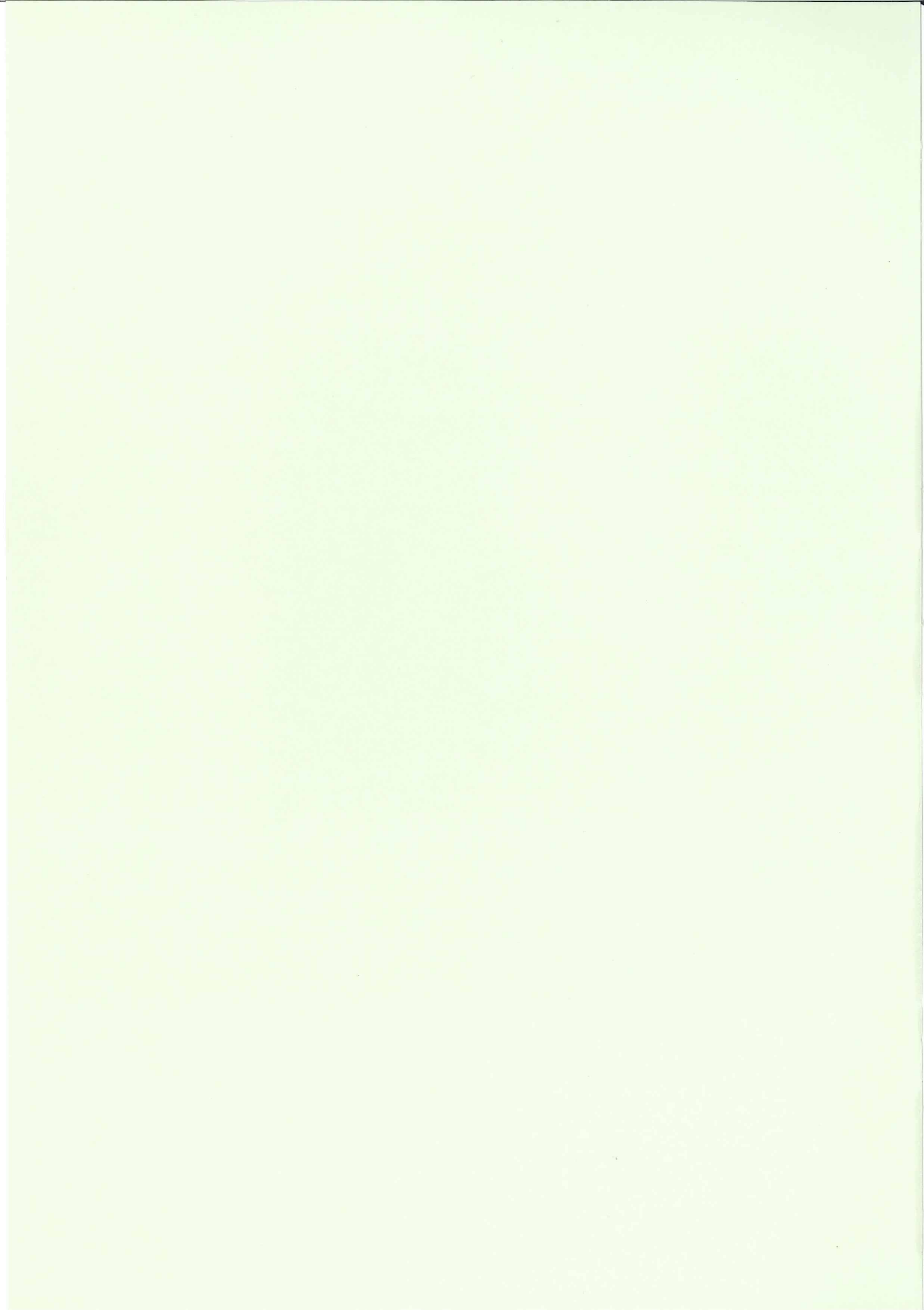
発表者氏名	論文タイトル名	発表誌名	巻号	ページ	出版年
Takahashi H, Takayama T, Yoneda K, Endo H, Iida H, Sugiyama M, Fujita K, Yoneda M, Inamori M, Abe Y, Saito S, Wada K, Nakagama H, Nakajima A	Association of visceral fat accumulation and plasma adiponectin with rectal dysplastic aberrant crypt foci in a clinical population	Cancer Sci.	100	29-32	2009
Paramasivam M, Membrino A, Cogoi S, Fukuda H, Nakagama H, Xodo LE	Protein hnRNP A1 and its derivative Up1 unfold quadruplex DNA in the human KRAS promoter: implications for transcription	Nucleic Acids Research	37	2841-2853	2009
Takahashi H, Takayama T, Hosono K, Yoneda K, Endo H, Nozaki Y, Fujita K, Yoneda M, Inamori M, Abe Y, Kobayashi N, Kirikoshi H, Kubota K, Saito S, Nakagama H, Nakajima A	Correlation of the plasma level of insulin-like growth factor-1 with the number of aberrant crypt foci in male individuals	Molecular Medicine Reports	2	339-343	2009

発表者氏名	論文タイトル名	発表誌名	巻号	ページ	出版年
Fukuda H, Takamura-Enya T, Masuda Y, Nohmi T, Seki C, Kamiya K, Sugimura T, Masutani C, Hanaoka F, Nakagama H	Translesional DNA synthesis through a C8-guanyl adduct of 2-amino-1-methyl-6-phenylimidazo[4,5-b]pyridine (PhIP) in vitro : REV1 inserts dC opposite the lesion, and DNA polymerase κ potentially catalyzes extension reaction from the 3'-dC terminus	Journal of Biological Chemistry	284	25585-25592	2009
Okamoto K, Taya Y, Nakagama H	Mdmx enhances p53 ubiquitination by altering the substrate preference of the Mdm2 ubiquitin ligase	FEBS Letters	583	2710-2714	2009
Endo H, Hosono K, Fujisawa T, Takahashi H, Sugiyama M, Yoneda K, Nozaki Y, Fujita K, Yoneda M, Inamori M, Wada K, Nakagama H, Nakajima A	Involvement of JNK pathway in the promotion of the early stage of colorectal carcinogenesis under high-fat dietary conditions	Gut	58	1637-1643	2009
Ohtsubo C, Shiokawa D, Kodama M, Gaiddon C, Nakagama H, Jochemsen AG, Taya Y, Okamoto K	Cytoplasmic tethering is involved in synergistic inhibition of p53 by Mdmx and Mdm2	Cancer Sci.	100	1291-1299	2009
Sugiyama M, Takahashi H, Hosono K, Endo H, Kato S, Yoneda K, Nozaki Y, Fujita K, Yoneda M, Wada K, Nakagama H, Nakajima A	Adiponectin inhibits colorectal cancer cell growth through the AMPK/mTOR pathway	International Journal of Oncology	3	339-344	2009
Uchida S, Yoshioka K, Kizu R, Nakagama H, Matsunaga T, Ishizaka Y, Poon RYC, Yamashita K	Stress-activated mitogen-activated protein kinases c-Jun NH2-terminal kinase and p38 target Cdc25B for degradation	Cancer Res.	69	6438-6444	2009
Shibata A, Maeda D, Ogino H, Tsutsumi M, Nohmi T, Nakagama H, Sugimura T, Teraoka H, Masutani M,	Role of Parp-1 in suppressing spontaneous deletion and mutation in the liver and brain of mice at adolescence and advanced age.	Mutation Research/Fundamental and Molecular Mechanisms of Mutagenesis	664	20-27	2009

発表者氏名	論文タイトル名	発表誌名	巻号	ページ	出版年
Shimokawa T, Ogino H, Maeda D, Nakagama H, Sugimura T, Masutani M,	Poly(ADP-ribose) preparation using anion-exchange column chromatography.	Organic Chemistry Insights	2	1-5	2009
Fujihara H, Ogino H, Maeda D, Shirai H, Nozaki T, Kamada N, Jishage K, Tanuma S, Takato T, Ochiya T, Sugimura T, Masutani M.	<i>Poly(ADP-ribose)</i> <i>glycohydrolase</i> deficiency sensitizes mouse ES cells to DNA damaging agents.	Curr Cancer Drug Targets	9	953-962	2009
Ogino H, Sakamoto H, Nakayama R, Yoshida T, Sugimura T, Masutani, M.	Analysis of the poly(ADP-ribose) polymerase-1 gene alteration in human germ cell tumor cell lines.	Cancer Genet Cytogenet.	197	8-15	2010
Kothe GO, Kitamura M, Masutani M, Selker EU, Inoue H	PARP is involved in replicative aging in <i>Neurospora crassa</i> .	Fungal Genet Biol.	47	297-309	2010
Akulevich NM, Saenko VA, Rogounovitch TI, Drozd VM, Lushnikov EF, Ivanov VK, Mitsutake N, Kominami R, Yamashita S.	Polymorphisms of DNA damage response genes in radiation-related and sporadic papillary thyroid carcinoma	Endocr. Relat. Cancer	16	491-503	2009
Nagamachi A, Yamasaki N, Miyazaki K, Oda H, Miyazaki M, Honda Z, Kominami R, Inaba T, Honda H.	Haploinsufficiency and acquired loss of Bcl11b and H2AX induces blast crisis of chronic myelogenous leukemia in a transgenic mouse model.	Cancer Sci.	100	1219-1226	2009
Yamamoto T, Morita S, Go E, Obata M, Katsuragi Y, Fujita Y, Maeda Y, Yokoyama M, Aoyagi Y, Ichikawa H, Mishima Y, Kominami R.	Clonally expanding thymocytes having lineage capability in γ -ray induced mouse atrophic thymus.	Int.J.Radiation Oncology Biol. Phys.	In press		
Go R, Hirose S, Morita S, Yamamoto T, Katsuragi Y, Mishima Y, Kominami R.	Bcl11b heterozygosity promotes clonal expansion and differentiation arrest of thymocytes in γ -irradiated mice.	Cancer Sci.	In press		
Oshima H, Itadani H, Kotani H, Taketo MM, Oshima M.	Induction of prostaglandin E2 pathway promotes gastric hamartoma development with suppression of bone morphogenetic protein signaling.	Cancer Res	69	2729-2733	2009

発表者氏名	論文タイトル名	発表誌名	巻号	ページ	出版年
Du YC, Oshima H, Oguma K, Kitamura T, Kitadani H, Fujimura T, Piao YS, Yoshimoto T, Minamoto T, Taketo MM, Oshima M.	Induction and downregulation of sox17 and its possible roles during the course of gastrointestinal tumorigenesis.	Gastroenterology	137	1346-1357	2009
Oshima H, Oguma K, Du YC, Oshima M.	Prostaglandin E2, Wnt and BMP in gastric tumor mouse models.	Cancer Sci	100	1779-1785	2009
Itadani H, Oshima H, Oshima M, Kotani H.	Mouse gastric tumor models with prostaglandin E2 pathway activation show similar gene expression profiles to intestinal-type human gastric cancer.	BMc Genomics	10	615	2009
Yoshimi K, Tanaka T, Takizawa A, Kato M, Hirabayashi M, Mashimo T, Serikawa T, Kuramoto T.	Enhanced colitis-associated colon carcinogenesis in a novel <i>Apc</i> mutant rat.	Cancer Sci.	100(11)	2022-2027	2009
Mashimo T, Takizawa A, Voigt B, Yoshimi K, Hiai H, Kuramoto T, Serikawa T.	Generation of knockout rats with X-linked severe combined immunodeficiency (X-SCID) using zinc-finger nucleases.	PLoS One	5(1)	e8870	2010
Oyama T, Yasui Y, Sugie S, and Tanaka T	Preclinical assays for identifying natural cancer chemopreventive agents.	Scholarly Research Exchange		1-15	2009
Oyama T, Yasui Y, Sugie S, Koketsu M, Watanabe K, Tanaka T	Dietary tricin suppresses inflammation-related colon carcinogenesis in male Crj: CD-1 mice.	Cancer Prev. Res.	2	1031-1038	2009
Endo H, Hosono K, Fujisawa T, Takahashi H, Sugiyama M, Yoneda K, Nozaki Y, Fujita K, Yoneda M, Inamori M, Wada K, Nakagama H, Nakajima A.	Involvement of JNK pathway in the promotion of the early stage of colorectal carcinogenesis under high-fat dietary condition.	Gut	58	1637-43	2009
Sugiyama M, Takahashi H, Hosono K, Endo H, Kato S, Yoneda K, Nozaki Y, Fujita K, Yoneda M, Wada K, Nakagama H, Nakajima A.	Adiponectin inhibits colorectal cancer cell growth through the AMPK/mTOR pathway.	Int J Oncol	34	339-44	2009

発表者氏名	論文タイトル名	発表誌名	巻号	ページ	出版年
Takahashi H, Takayama T, Yoneda K, Endo H, Iida H, Sugiyama M, Fujita K, Yoneda M, Inamori M, Abe Y, Saito S, Wada K, Nakagama H, Nakajima A	Association of visceral fat accumulation and plasma adiponectin with rectal dysplastic aberrant crypt foci in a clinical population.	Cancer Sci	100	29-32	2009



平成21年度 厚生労働科学研究費補助金
第3次対がん総合戦略研究事業 中签班
総括・分担研究報告書 2/2冊

疾患モデル動物を用いた環境発がんの初期発生過程及び感受性要因の
解明とその臨床応用に関する研究

中签 斉

Translesional DNA Synthesis through a C8-Guanyl Adduct of 2-Amino-1-methyl-6-phenylimidazo[4,5-*b*]pyridine (PhIP) *in Vitro*

REV1 INSERTS dC OPPOSITE THE LESION, AND DNA POLYMERASE κ POTENTIALLY CATALYZES EXTENSION REACTION FROM THE 3'-dC TERMINUS^{*[5]}

Received for publication, June 25, 2009, and in revised form, July 16, 2009. Published, JBC Papers in Press, July 23, 2009, DOI 10.1074/jbc.M109.037259

Hirokazu Fukuda[‡], Takeji Takamura-Enya[§], Yuji Masuda[¶], Takehiko Nohmi^{||}, Chiho Seki[‡], Kenji Kamiya[§], Takashi Sugimura[†], Chikahide Masutani^{**}, Fumio Hanaoka^{**1}, and Hitoshi Nakagama^{‡2}

From the [‡]Biochemistry Division, National Cancer Center Research Institute, 1-1, Tsukiji 5, Chuo-ku, Tokyo 104-0045, the [§]Department of Applied Chemistry, Faculty of Engineering, Kanagawa Institute of Technology, Ogino 1030, Atsugi, Kanagawa 243-0292, the [¶]Department of Experimental Oncology, Research Institute for Radiation Biology and Medicine, Hiroshima University, Kasumi 1-2-3, Minami-ku, Hiroshima, Hiroshima 734-8553, the ^{||}Division of Genetics and Mutagenesis, National Institute of Health Sciences, Kamiyoga 1-18-1, Setagaya-ku, Tokyo 158-8501, and the ^{**}Cellular Biology Laboratory, Graduate School of Frontier Biosciences, Osaka University, Yamada-oka 1-3, Suita, Osaka 565-0871, Japan

2-Amino-1-methyl-6-phenylimidazo[4,5-*b*]pyridine (PhIP) is the most abundant heterocyclic amine in cooked foods, and is both mutagenic and carcinogenic. It has been suspected that the carcinogenicity of PhIP is derived from its ability to form DNA adducts, principally dG-C8-PhIP. To shed further light on the molecular mechanisms underlying the induction of mutations by PhIP, *in vitro* DNA synthesis analyses were carried out using a dG-C8-PhIP-modified oligonucleotide template. In this template, the dG-C8-PhIP adduct was introduced into the second G of the TCC GGG AAC sequence located in the 5' region. This represents one of the mutation hot spots in the rat *Apc* gene that is targeted by PhIP. Guanine deletions at this site in the *Apc* gene have been found to be preferentially induced by PhIP in rat colon tumors. DNA synthesis with A- or B-family DNA polymerases, such as *Escherichia coli* polymerase (pol) I and human pol δ , was completely blocked at the adducted guanine base. Translesional synthesis polymerases of the Y-family, pol η , pol ι , pol κ , and REV1, were also used for *in vitro* DNA synthesis analyses with the same templates. REV1, pol η , and pol κ were able to insert dCTP opposite dG-C8-PhIP, although the efficiencies for pol η and pol κ were low. pol κ was also able to catalyze the extension reaction from the dC opposite dG-C8-PhIP, during which it often skipped over one dG of the triple dG sequence on the template. This slippage probably leads to the single dG base deletion in colon tumors.

Heterocyclic amines (HCAs)³ are naturally occurring genotoxic carcinogens produced from cooking meat (1). The initial

carcinogenic event induced by HCAs is metabolic activation and subsequent covalent bond formation with DNA (1, 2). 2-Amino-1-methyl-6-phenylimidazo[4,5-*b*]pyridine (PhIP) is the most abundant heterocyclic amine in cooked foods, and was isolated from fried ground beef (3, 4). PhIP possesses both mutagenic and carcinogenic properties (5–8). Epidemiological studies have revealed that a positive correlation exists between PhIP exposure and mammary cancer incidence (9). PhIP induces colon and prostate cancers in male rats and breast cancer in female rats (8, 10).

The incidences of colon, prostate, and breast cancers are steadily increasing in Japan and other countries and this has been found to correlate with a more Westernized lifestyle. Elucidating the molecular mechanisms underlying PhIP-induced mutations is therefore of considerable interest. It is suspected that the carcinogenicity of PhIP is derived from the formation of DNA adducts, principally dG-C8-PhIP (11–14) (see Fig. 1). Studies of the mutation spectrum of PhIP in mammalian cultured cells and transgenic animals have revealed that G to T transversions are predominant and that guanine deletions from G stretches, especially from the 5'-GGGA-3' sequence, are significant (15–20). Five mutations in the *Apc* gene were detected in four of eight PhIP-induced rat colon tumors, and all of these mutations involved a single base deletion of guanine from 5'-GGGA-3' (21). These mutation spectra are thought to be influenced by various factors, including the primary structure of the target gene itself, the capacity of translesional DNA polymerases, and the activity level of repair enzymes (1). However, the molecular mechanisms underlying the formation of PhIP-induced mutations are largely unknown.

To shed further light on the molecular processes that underpin the mutations induced by PhIP, we performed *in vitro* DNA synthesis analyses using a dG-C8-PhIP-modified oligonucleotide template. We have recently reported the successful synthesis of oligonucleotides harboring a site-specific PhIP adduct

dithiothreitol; PCNA, proliferating cell nuclear antigen; PIPES, 1,4-piperazine diethanesulfonic acid.

* This work was supported by Kakenhi Grant 19570144.

[5] The on-line version of this article (available at <http://www.jbc.org>) contains supplemental Table S1 and Figs. S1–S6.

¹ Present address: Dept. of Life Science, Faculty of Science, Gakushuin University, Mejiro 1-5-1, Toshima-ku, Tokyo 171-8588, Japan.

² To whom correspondence should be addressed. Tel.: 81-3-3542-2511; Fax: 81-3-3542-2530; E-mail: hnakagam@ncc.go.jp.

³ The abbreviations used are: HCA, heterocyclic amines; PhIP, 2-amino-1-methyl-6-phenylimidazo[4,5-*b*]pyridine; TLS, translesional DNA synthesis; IQ, 2-amino-3-methylimidazo[4,5-*f*]quinoline; pol, DNA polymerase; DTT,

Translesional Synthesis through the dG-C8-PhIP Adduct

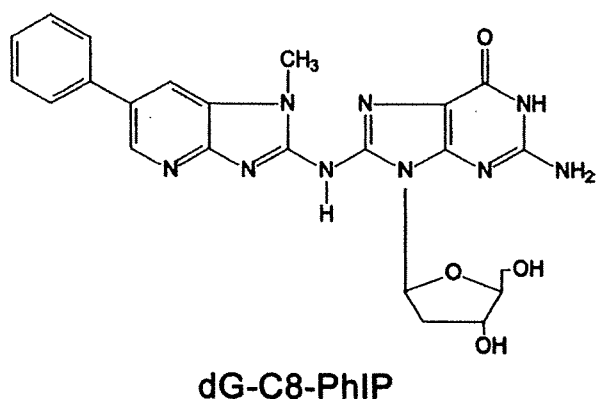


FIGURE 1. Structure of the dG-C8-PhIP adduct.

(22). In our current study, we used this synthesis method to construct a 32-mer oligonucleotide template containing a 5'-TTCGGGAAC-3' sequence with different site-specific PhIP adducts. We then utilized the resulting constructs in DNA synthesis analyses to reconstitute the PhIP-induced mutagenesis of the rat *APC* gene. DNA synthesis reactions with A- or B-family DNA polymerases, such as *Escherichia coli* pol I and human pol δ , or translesional synthesis (TLS) polymerases of the Y-family, pol η , pol ι , pol κ , and REV1, were carried out. Kinetic analyses of pol κ and REV1, for which TLS activities at the PhIP adduct were detected, were also performed.

EXPERIMENTAL PROCEDURES

Enzymes and Materials—T4 polynucleotide kinase and T4 DNA ligase were purchased from Toyobo Biochem (Osaka, Japan) and Takara Biotech (Tokyo, Japan), respectively. Other materials were obtained from Sigma or Wako (Osaka, Japan).

DNA Polymerases and PCNA—Human recombinant DNA polymerases, pol δ , pol η , pol κ , and REV1, and PCNA were expressed and purified as described previously (23–27). Human DNA polymerase α and DNA polymerase ι were purchased from Chimex. *E. coli* DNA polymerases I (Takara Biotech) and Klenow Fragment (Takara Biotech), and thermophilic bacterial DNA polymerases, *rTaq* (Toyobo Biochem) and *Tth* (Toyobo Biochem) were used.

Oligonucleotides—The method used to chemically synthesize three 9-mer oligonucleotides, 5'-TCCGGGAAC-3', containing a PhIP adduct on either the first, second, or third G (p9B, p9C, and p9D, respectively) has been described previously (22). All other synthetic oligonucleotides were synthesized and purified using a reverse-phase cartridge (Operon Biotech Japan (Tokyo, Japan)). The 23-mer oligonucleotides: p23a, 5'-TGAC-TCGTCGTGACTGGGAAAAC-3', and p23b, 5'-GTCACGACGAGTCAGTTCCTCGGA-3', were used for constructing the template oligonucleotides as described below. A 32-mer oligonucleotide without the PhIP adduct, p32A, was used as a control template (see Table 1). Its 3' complementary 29-, 28-, 27-, 26-, 22-, and 17-mer sequences (p29, p28, p27, p26, p22, and p17) were used as extension primers (see Table 1).

Construction of Template-Primer Complexes Containing the PhIP Adduct—A 32-mer template oligonucleotide p32C (see Table 1) was constructed by ligation of p9C with p23a as follows. The 5'-end of p23a was phosphorylated by T4 polynucle-

otide kinase and ATP. A mixture of p9C, p23a, and p23b (3 nmol each) in 250 μ l of a buffer containing 5 mM Tris-HCl, 0.5 mM EDTA, 50 mM NaCl, pH 8.0, was denatured for 5 min at 95 $^{\circ}$ C, incubated for 10 min at 60 $^{\circ}$ C, and then cooled slowly to form the partial duplex structure of these three oligonucleotides (supplemental Fig. S1). The sample of the duplex oligonucleotide was mixed with 190 μ l of Milli-Q water and 50 μ l of $\times 10$ ligation buffer (500 mM Tris-HCl (pH 7.5), 100 mM MgCl₂, 100 mM DTT, 10 mM ATP). Ligation was initiated by adding 10 μ l of T4 DNA ligase (4,000 units), and the mixture was then incubated for 20 h at 16 $^{\circ}$ C. An additional incubation at 37 $^{\circ}$ C for 60 min was carried out after the addition of 1 μ l of T4 DNA ligase, and the reaction was stopped by further incubation at 68 $^{\circ}$ C for 10 min. The p32C was separated by 18% PAGE containing 8 M urea, and excised and eluted as described previously (28). p32B and p32D were constructed using a similar method as for p9B and p9D, respectively (see Table 1). The purities of these oligonucleotides, p32B, p32C, and p32D, were determined by denatured PAGE after 5'-end labeling and UV absorbance at 260 and 370 nm.

Primer oligonucleotides were labeled with ³²P at the 5'-end as described previously (29), and then purified by MicroSpinTM G-25 or G-50 columns (GE Healthcare) as recommended by the supplier. The mixture of template and labeled primer (50 pmol each) in 400 μ l of a buffer containing 8 mM Tris-HCl, 0.8 mM EDTA, 150 mM KCl (pH 8.0) was heated at 70 $^{\circ}$ C for 7 min, and then cooled slowly to room temperature. In the case of the substrates for TLS polymerases, pol η , pol ι , pol κ , and REV1, the final concentrations of template-primer and the constituents of the annealing buffers were changed to 500 nM and 10 mM Tris-HCl, 1 mM EDTA, and 50 mM NaCl (pH 8.0), respectively.

In Vitro DNA Synthesis Assay—A primer extension reaction was performed as described previously (30) with some modifications. Briefly, an aliquot of 0.75 μ l of this primer-annealed template (final concentration, 12.5 nM) was mixed with 0.75 μ l of $\times 10$ Klenow buffer (100 mM Tris-HCl (pH 7.5), 70 mM MgCl₂, 1 mM DTT), 0.5 μ l of 500 mM KCl, 0.5 μ l of dNTP mixture (50 μ M each), and 4.5 μ l of Milli-Q water. After addition of 0.5 μ l of Klenow fragment, the mixture was incubated at 37 $^{\circ}$ C for 10 min. The reaction was terminated by adding 1.5 μ l of stop solution (160 mM EDTA, 0.7% SDS, 6 mg/ml proteinase K), and the samples were incubated at 37 $^{\circ}$ C for 30 min. Subsequently, 5.5 μ l of the gel loading solution (30 mM EDTA, 0.05% bromophenol blue, 0.05% xylene cyanol, 97% formamide) was added to the samples. For pol δ , a $\times 10$ reaction buffer containing 200 mM PIPES (pH 6.8), 20 mM MgCl₂, 10 mM 2-mercaptoethanol, 200 μ g/ml bovine serum albumin, and 50% glycerol was used instead of the buffer described above, and the reaction was carried out at 37 $^{\circ}$ C for 10 min. For other DNA polymerases, pol α , pol I, *rTaq*, and *Tth*, the constituent of each $\times 10$ reaction buffer was altered as recommended by the suppliers.

The reaction using pol κ was performed as described above with some modifications. Briefly, an aliquot of 0.5 μ l of this primer-annealed template (final 50 nM) was mixed with 0.5 μ l of $10 \times$ TLS buffer (250 mM Tris-HCl (pH 7.0), 50 mM MgCl₂, 50 mM DTT, 1 mg/ml bovine serum albumin), 0.5 μ l of dNTP solution, and 3.0 μ l of Milli-Q water. After addition of 0.5 μ l of pol κ , the mixture was incubated at 30 $^{\circ}$ C for 20 min. The reac-

Translesional Synthesis through the dG-C8-PhIP Adduct

tion was terminated by adding 8.8 μ l of the gel loading solution and a further incubation at 95 °C for 3 min. The reaction of REV1 was performed in the same manner as the reaction of pol κ with the exception that the standard reaction time was 5 min. For pol η , a $\times 10$ reaction buffer containing 400 mM Tris-HCl (pH 8.0), 10 mM MgCl₂, 100 mM DTT, 1 mg/ml bovine serum albumin, and 450 mM KCl was used instead of the $\times 10$ TLS buffer. The ³²P-labeled fragments were denatured and electrophoresed in a 9.5% polyacrylamide gel containing 8 M urea. The radioactivity of the fragments was determined using a Bio-Imaging Analyzer (BAS2500, Fuji Photo Film, Kanagawa, Japan). Kinetic parameters were determined by steady-state gel kinetic assays under similar conditions as described above. The incubation time for pol κ was changed to 10 min. K_m and k_{cat} were evaluated from the plot of the initial velocity versus the dCTP or dGTP concentration using a hyperbolic curve-fitting program in SigmaPlot 11 (Systat Software, Inc.). Data from two or three independent experiments were plotted together.

RESULTS

Construction of Template Oligonucleotides Containing a PhIP Adduct—We designed oligonucleotides containing a dG-C8-PhIP adduct at specific sites for use as templates in *in vitro* DNA synthesis analyses. For this purpose, we selected the 5'-TCCGGGAAC-3' sequence as: 1) it corresponds to codon 868–870 of the rat *Apc* gene, one of three mutation hot spots (a single base deletion of G) in PhIP-induced colon tumors (21), and could thus be used as a model template that would reconstitute mutations of this gene; 2) two other mutation hot spots in the rat *Apc* gene and many mutated sites induced by PhIP in cultured cells and animal models contain 5'-GGGA-3' as a core sequence (17–20). We thus speculated that the 5'-TCCGGGAAC-3' sequence could be used as a model sequence for these GGGGA to GGA mutations to some extent; and 3) some mutagenic compounds forming dG adducts, including PhIP, are expected to react preferentially with the 5'-G of a GG dinucleotide site when compared with a single G residue (31). We thus selected a sequence containing GGG as a template for our initial analysis.

We have recently synthesized three 9-mer oligonucleotides separately harboring a PhIP adduct on each G within the sequence 5'-TCC GGG AAC-3' (22). Three 32-mer template oligonucleotides, p32B, p32C, and p32D, were constructed in our present study by ligation of these 9-mer oligonucleotides containing the dG-PhIP adduct with a 23-mer oligonucleotide, p23a, (Table 1 and supplemental Fig. S1). The purities of these oligonucleotides were tested after resolution by electrophoresis. In our present study, we principally describe the results of our *in vitro* DNA synthesis analysis using p32C as the template to avoid complexity.

In Vitro DNA Synthesis by A- and B-family DNA Polymerase—Many of the chemical compounds that can form DNA adducts *in vivo* and that show mutagenicity have been reported to impede the progress of DNA synthesis to different extents. The molecular size of PhIP is greater than most other mutagenic chemicals that form adducts. Hence, dG-PhIP was expected to block DNA synthesis to a considerable extent. To examine the effects of the dG-C8-PhIP adduct upon DNA synthesis, primer

TABLE 1
Oligonucleotide templates and primers

Oligonucleotide	Sequence ^a
p32A	5'-TCC <u>GGG</u> AAC TGACTCGTC GTGACTGGG AAAAC-3'
p32B	5'-TCC <u>GGG</u> AAC TGACTCGTC GTGACTGGG AAAAC-3'
p32C	5'-TCC <u>GGG</u> AAC TGACTCGTC GTGACTGGG AAAAC-3'
p32D	5'-TCC <u>GGG</u> AAC TGACTCGTC GTGACTGGG AAAAC-3'
p29	5'-GTT TTC CCA GTCACGACG AGTCAGTTC CC-3'
p28	5'-GTT TTC CCA GTCACGACG AGTCAGTTC C-3'
p27	5'-GTT TTC CCA GTCACGACG AGTCAGTTC-3'
p26	5'-GTT TTC CCA GTCACGACG AGTCAGTTC-3'
p22	5'-GTT TTC CCA GTCACGACG AGTC-3'
p17	5'-GTT TTC CCA GTCACGAC-3'

^a The bold G indicates the site of the PhIP-C8-dG adduct. Underlined sequences correspond to codon 868–870 at nucleotides 2602–2610 of the rat APC gene.

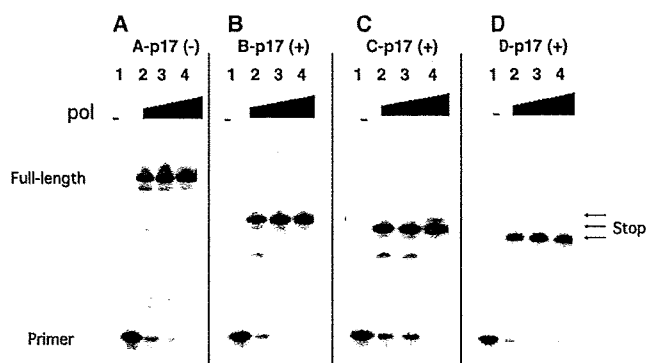


FIGURE 2. *In vitro* DNA synthesis using Klenow fragment. Gel electrophoresis indicating the primer extensions obtained using the 32-mer oligonucleotide templates, p32A (A), p32B (B), p32C (C), and p32D (D), which have no PhIP adduct, and a PhIP adduct on the first, second, and third G within the triple G sequence, respectively. The 3' complementary 17-mer sequence, p17, was used as the extension primer. The final concentration of each template-primer complex was 12.5 nM. Concentrations of Klenow fragment were 0 (lane 1), 7.8 (lane 2), 23 (lane 3), and 78 units/ml (lane 4).

extension experiments using p32B, p32C, and p32D as templates were carried out (see Table 1). The length of each produced fragment was precisely determined using ladders of oligonucleotide fragments as markers (data not shown). The Klenow fragment of *E. coli* DNA polymerase I, a member of the A-family DNA polymerases, was first used in this analysis. The production of a 28-, 27-, and 26-mer from these primer extension reactions using B-p17, C-p17, and D-p17, respectively, using a template-primer complex, and lack of longer fragments indicated that the Klenow fragment stalled just before the dG-C8-PhIP adduct (Fig. 2). On the other hand, control experiments using p32A without the adduct as a template produced a 32-mer fragment (Fig. 2A). Similar results were obtained with *E. coli* DNA polymerase I (exo⁺) and B-family DNA polymerases, such as the thermophilic bacterial DNA polymerases, *rTaq* and *Tth*, and human DNA polymerase α (data not shown) (supplemental Fig. S2), suggesting that stalling at the dG-C8-PhIP adduct occurs for all replicative DNA polymerases. Stalling of *rTaq* and *Tth* at the PhIP adduct was observed at 65 °C, as well as at 37 °C, indicating that this is the result of a physical hindrance of the adduct itself and not from secondary DNA structures. Moreover, there was no difference found between the stalling of *E. coli* DNA polymerase I (exo⁺) and that of the Klenow fragment (exo⁻). This indicates that the physical blocking of DNA polymerases at the dG-C8-PhIP adduct does not depend upon their proofreading function.

Translesional Synthesis through the dG-C8-PhIP Adduct

Finally, DNA synthesis analyses with human DNA polymerase δ (pol δ), a member of the B-family DNA polymerases and a truly replicative polymerase, were carried out. In the case of

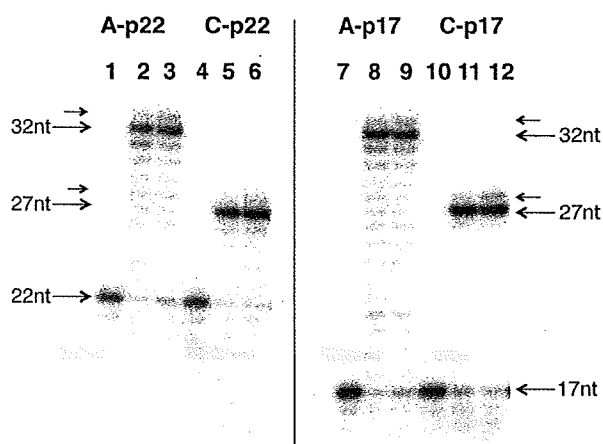


FIGURE 3. *In vitro* DNA synthesis using pol δ in the presence or absence of PCNA. Gel electrophoresis indicating the primer extensions obtained using the 32-mer oligonucleotide templates, p32A (A), and p32C (C), which have no PhIP adduct, and a PhIP adduct on the second G within the triple G sequence, respectively. The 3' complementary 22- and 17-mer sequences, p22 and p17, were used as the extension primer. The final concentration of each template-primer complex was 12.5 nM. Concentrations of pol δ were 0 (lanes 1, 4, 7, and 10) and 16 nM (lanes 2, 3, 5, 6, 8, 9, 11, and 12). Concentrations of PCNA as a trimer were 0 (lanes 1, 2, 4, 5, 7, 8, 10, and 11) and 20 nM (lanes 3, 6, 9, and 12). Large arrows indicate the positions of primers (17- or 22-mer), full-length products (32-mer), and the products pausing just before the PhIP adduct (27-mer). Small arrows indicate the minor products that incorporated an additional 1 nucleotide (nt) to a full-length product or the pausing product.

using p32C and p17 (C-p17) as a template-primer complex, the production of 27-mer fragments indicated the stalling of pol δ just before the PhIP adduct (Fig. 3, lane 11). From a control reaction using A-p17, a template-primer complex without the PhIP adduct, a full-length product of 32-mer was generated (Fig. 3, lane 8). In addition to these major products, minor products extended one nucleotide further (28- and 33-mer) and ladders of bands indicating degradation of primer (<17-mer) were observed (Fig. 3), corresponding with previous results reporting terminal dA transferase and exonuclease activities of pol δ (32). PCNA, an accessory protein acting as a sliding clamp for pol δ , was previously reported to promote DNA synthesis by pol δ past several template lesions, including abasic sites, 8-oxo-dG, and aminofluorene-dG (32). In the case of dG-C8-PhIP, however, PCNA was unable to promote the bypass synthesis of pol δ beyond the lesion (Fig. 3, lane 12). Extension reaction from the longer 22-mer primer, p22, also paused completely just before the PhIP adduct in the presence or absence of PCNA (Fig. 3, lanes 5 and 6). These results strongly suggest that the dG-C8-PhIP adduct on genome DNA in the living cells induces the complete block of replication forks including pol δ , PCNA, and pol α .

Translesional DNA Synthesis by Y-family DNA Polymerases— Translesional DNA synthesis at the dG-C8-PhIP adduct by the Y-family DNA polymerases, pol η , pol κ , pol ι , and REV1 was next examined. Two substrates, C-p27 and C-p28, and their counterparts without a PhIP adduct, A-p27 and A-p28, were used in these experiments (Fig. 4). Substrate C-p27 was prepared by annealing the p32C template (see Table 1) to its 3'-complementary 27-mer sequence, p27, and was used to identify the nucleotides that are inserted

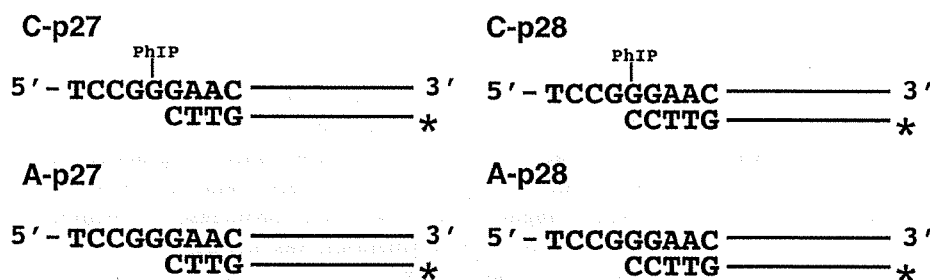


FIGURE 4. Template-primer complexes. Substrates C-p27 and C-p28 (series-C) have a PhIP adduct on the second dG within a GGG sequence. Substrates A-p27 and A-p28 (series-A) are control substrates without a PhIP adduct. The corresponding 3' complementary 27- and 28-mer sequences, p27 and p28, were used as extension primers. The template-primer complexes, C-p27 and C-p28, were used to monitor the nucleotide insertions into the site opposite dG-C8-PhIP and the extension reactions from the 3'-dC opposite dG-C8-PhIP, respectively.

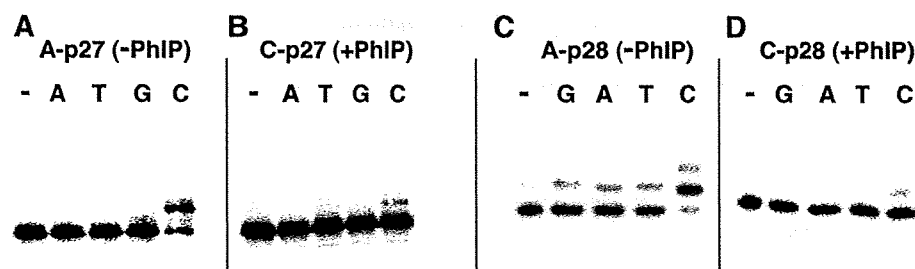


FIGURE 5. Translesional DNA synthesis by pol η using substrates C-p27 and C-p28. Control reactions were performed using substrates without the PhIP adduct, A-p27 (A) and A-p28 (C). An insertion reaction was performed with substrate C-p27 (B) and an extension reaction with substrate C-p28 (D). A single dNTP (G, A, T, C) was added into the reaction mixture as indicated by G, A, T, and C above each lane. The lanes indicated by - are controls without any nucleotides. Concentrations of pol η and each dNTP were 1.9 nM and 100 μ M, respectively.

opposite the dG-C8-PhIP adduct (Fig. 4). Similarly, substrate C-p28 was used to analyze the extension reaction from the 3'-end of the dC bases opposite the dG-C8-PhIP adduct (Fig. 4). We found that recombinant human DNA polymerase η (pol η) could insert a dC opposite the dG-C8-PhIP adduct, although at low efficiency compared with control experiments without the PhIP adduct (Fig. 5, A and B). Extension reactions catalyzed by pol η from the 3'-end of dC opposite the adduct were barely detectable (Fig. 5D), although an excessive amount of pol η produced byproducts that incorporated a mismatch nucleotide, dG, dA, or dT (supplemental Fig. S4). In the case of dG, incorporation of one to three dG nucleotides was observed (supplemental Fig. S4). In control experiments without the PhIP adduct, minor products were produced that incorporated mismatch nucleotides, in addition to a major product that incorporated a dC (Fig. 5C).

Translesional Synthesis through the dG-C8-PhIP Adduct

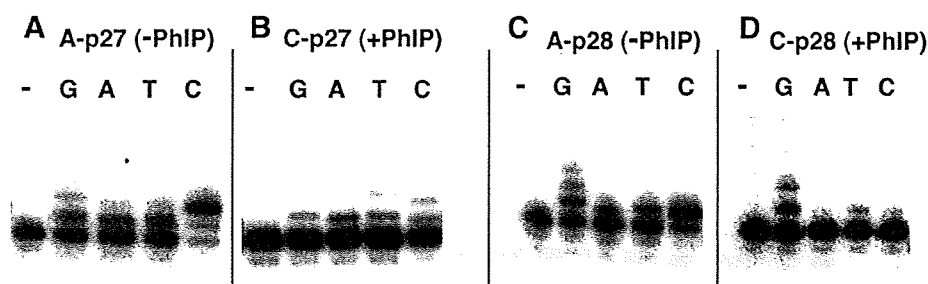


FIGURE 6. Translesional DNA synthesis by pol κ using substrates C-p27 and C-p28. Control reactions were performed using substrates without the PhIP adduct, A-p27 (A) and A-p28 (C). An insertion reaction was performed with substrate C-p27 (B) and an extension reaction with substrate C-p28 (D). A single dNTP (G, A, T, C) was added into the reaction mixture as indicated by G, A, T, and C above each lane. The lanes indicated by – are controls without any nucleotides. The concentrations of pol κ were 250 (A and C), 500 (B), and 1000 nM (D), respectively. The concentration of each dNTP was 100 μ M.

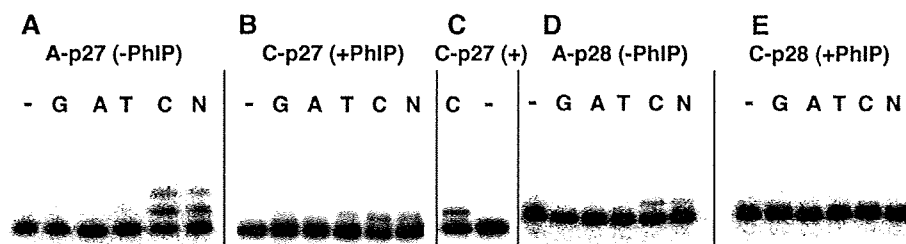


FIGURE 7. Translesional DNA synthesis by REV1 using substrates C-p27 and C-p28. Control reactions were performed using substrates without the PhIP adduct, A-p27 (A) and A-p28 (D). Insertion reactions were performed with substrate C-p27 (B and C) and an extension reaction with substrate C-p28 (E). A single dNTP (G, A, T, and C) or a mixture of each was added into the reaction mixture as indicated by G, A, T, C, and N above each lane. The lanes indicated by – are controls without any nucleotides. The concentrations of REV1 were 5.2 (A and D) and 26 nM (B, C, and E), respectively. The concentrations of each dNTP were 100 μ M (A, B, D, and E) and 320 μ M (C), respectively. The N mixture contained each dNTP at a concentration of 25 μ M.

We next examined translesional DNA synthesis beyond the PhIP adduct using a truncated form of human DNA polymerase κ containing the N-terminal 559 amino acids. One or two dCs were inserted opposite the dG-C8-PhIP adduct by this polymerase, and misinsertions of three other nucleotides were also observed to a certain extent (Fig. 6B). pol κ incorporated two dCs and misincorporated dG, dA, and dT into the A-p27 substrate without the PhIP adduct at a low efficiency (Fig. 6A). Misincorporations of dG, dA, and dT into the A-p28 substrate without the adduct were also observed (Fig. 6C). In the case of the extension reaction from 3'-dC opposite the dG-PhIP adduct, pol κ also incorporated dC and misincorporated dT into the C-p28 substrate at low efficiency (Fig. 6D). Interestingly, one- and two-base incorporations of dG into the substrate C-p28 by pol κ dominated the incorporation of a dC (Fig. 6D). In the extension reaction with pol κ in the presence of all four dNTPs, fragments of 29 and 30 nucleotides were observed as major products, and a small amount of the 31-nucleotide fragment was observed (see supplemental Fig. S5, lane 6). Full-length products of 32 nucleotides were observed only when an excess amount of pol κ was present (data not shown). This poor extension activity of pol κ after adding two nucleotides was probably caused by the shortness (\sim 4 nucleotides) of the 5' region to the lesion in the template oligonucleotide. Extension with pol κ , pol η , and pol δ from the mismatched primers, where the 3'-terminal nucleotide of the p28 primer, dC, was substituted with another nucleotide, could not be observed (data not shown). REV1 inserted a dC opposite the PhIP adduct

at a higher efficiency compared with pol κ and pol η (Fig. 7, B and C). REV1 was, however, unable to catalyze the extension reaction from the dC opposite the PhIP adduct in C-p28 (Fig. 7E and supplemental Fig. S5, lane 5). REV1 incorporated only dC nucleotides into A-p27 and A-p28 substrates without the adduct (Fig. 7, A and D). Neither nucleotide insertion nor extension reactions for the templates containing the PhIP adduct were detected using human pol ι (data not shown).

Kinetic Analyses of Translesional DNA Synthesis by pol κ and REV1—

To evaluate translesional DNA synthesis beyond the dG-C8-PhIP adduct in further detail, additional quantitative analyses for pol κ and REV1 were performed. Insertion reactions catalyzed by pol κ for dC (Fig. 8, B, lanes 2–5, and C, closed diamonds) and dG (Fig. 8, B, lanes 6–9, and C, closed triangles) into substrate C-p28 were analyzed in the same way. Kinetic parameters for pol κ were determined using steady-state kinetic assays (Table 2).

The catalytic efficiency (k_{cat}/K_m) of dC insertion into C-p28 (0.039 $\text{min}^{-1} \text{mM}^{-1}$) was found to be 4-fold greater than that into C-p27 (0.011 $\text{min}^{-1} \text{mM}^{-1}$). These results indicate that pol κ catalyzes the extension reaction from the 3'-terminal of dC opposite the dG-C8-PhIP with a higher efficiency than the insertion reaction opposite the adduct. The k_{cat}/K_m values of the dC insertion opposite the adduct were roughly 4 orders of magnitude less than those into counterparts without the adduct (see Table 2). The k_{cat}/K_m value of the dG incorporation into C-p28 was slightly higher than that of dC, and more than 8-fold higher than that of dG into C-p27 (see Table 2). This result indicates that pol κ skipped over the dG site just 5' of dG-C8-PhIP on the template and incorporated dG opposite dC on the template strand of substrate C-p28 with a high efficiency. The k_{cat}/K_m values of the dC incorporation into D-p27 (0.19 $\text{min}^{-1} \text{mM}^{-1}$) were over 4-fold greater than into C-p28 (0.039 $\text{min}^{-1} \text{mM}^{-1}$) and over 8-fold higher than that of dG into B-p29 (0.023) (see supplemental Table S1). These data indicate that the efficiencies of the extension reaction by pol κ are the highest for template p32D containing the PhIP adduct in the third G of the triple G run, next for template p32C containing the PhIP/adduct in the second G, and lowest for template p32B containing the PhIP adduct in the first G.

Even at higher concentrations of dNTPs, extension reactions catalyzed by REV1 for substrate C-p28 could not be monitored (Table 3, Fig. 7E). The k_{cat}/K_m value of the dC incorporation by REV1 into substrate C-p27 was more than 2,000 times greater than that by pol κ , and 1/44 of the values for counterparts with-

Translesional Synthesis through the dG-C8-PhIP Adduct

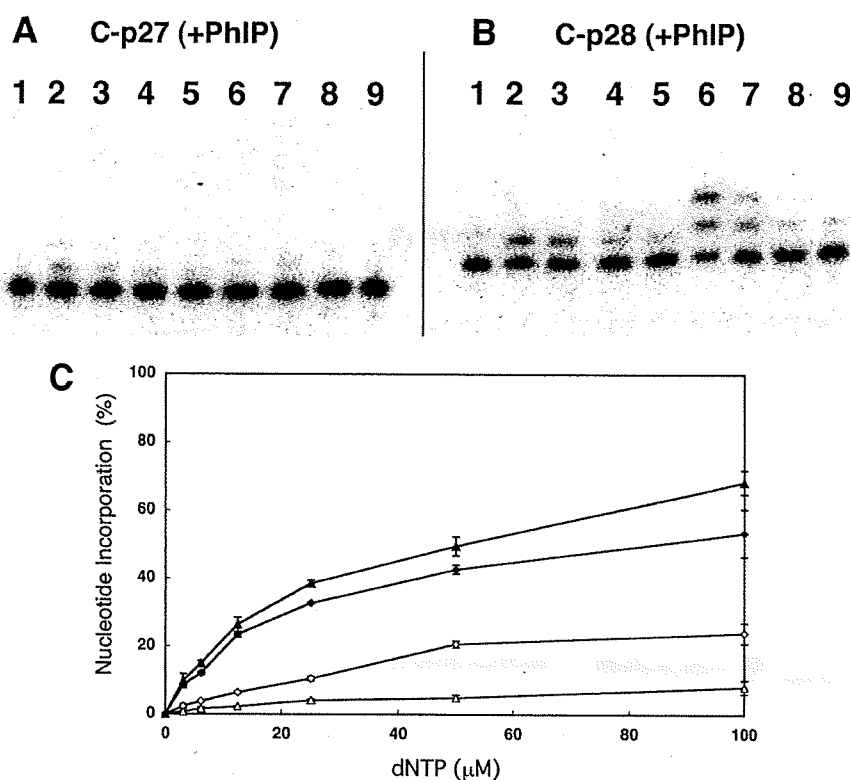


FIGURE 8. Translesional DNA synthesis by pol κ . Nucleotide incorporation by pol κ for substrates C-p27 (A) and C-p28 (B). Either dCTP (lanes 2-5) or dGTP (lanes 6-9) was added into the reaction mixture. Lane 1 indicates a control without any nucleotides. The concentration of pol κ was 910 nM. The concentrations of dCTP or dGTP, respectively, were 25 (lanes 2 and 6), 12.5 (lanes 3 and 7), 6.25 (lanes 4 and 8), and 3.13 μM (lanes 5 and 9). C, incorporation efficiencies of dCTP and dGTP into substrate C-p27 and C-p28. Incorporations of dCTP into C-p27, dGTP into C-p27, dCTP into C-p28, and dGTP into C-p28 are indicated by open diamonds, open triangles, closed diamonds, and closed triangles, respectively. Each data point represents the mean of two separate experiments. The error bars represent residuals.

TABLE 2
 k_{cat}/K_m values for pol κ

Substrate	K_m μM	k_{cat} $\times 10^{-3} \text{ min}^{-1}$	k_{cat}/K_m $\text{min}^{-1} \text{ mM}^{-1}$
C-p27			
dCTP	70	0.76	0.011
dGTP	47	0.24	0.0050
C-p28			
dCTP	8.0	0.32	0.039
dGTP	11	0.48	0.042
A-p27			
dCTP	0.035	4.4	130
dGTP	0.26	1.3	5.0
A-p28			
dCTP	0.027	3.7	140
dGTP	2.1	8.8	4.1

TABLE 3
 k_{cat}/K_m values for dCTP-insertion by REV1

Substrate	K_m μM	k_{cat} $\times 10^{-3} \text{ min}^{-1}$	k_{cat}/K_m $\text{min}^{-1} \text{ mM}^{-1}$
C-p27	12	320	27
C-p28	ND ^a	ND	ND
A-p27	0.36	390	1100

^a ND, not detectable.

out the adduct (Table 3). The k_{cat}/K_m values of the dC insertion by REV1 into three substrates, B-p28, C-p27 and D-p26, were 39, 27, and 73 $\text{min}^{-1} \text{ mM}^{-1}$, respectively. Thus, the insertion

reaction catalyzed by REV1 among the three templates was the most efficient for template p32D containing the PhIP adduct at the third G, similar to the extension reaction by pol κ .

DISCUSSION

In Vitro TLS Analysis Reconstituting PhIP-induced Mutations—HCAs are food-borne carcinogens produced when cooking meat (1, 9, 33). The most significant aspect of these molecules is that they exist normally in cooked food and are thus ubiquitous carcinogens (32). The mutagenicity and carcinogenicity of HCAs are mainly attributed to C8- and N2-dG adducts (9). Both excision repair and translesional DNA synthesis play critical roles in the mutagenesis steps induced by HCAs. However, despite the importance of HCAs as common environmental mutagens, there have been very few previous reports regarding the stalling of DNA polymerases and TLS caused by the DNA adducts they form. This is mainly because of the difficulty in preparing template DNA with introduced HCA adducts at specific sites. Choi *et al.*

(34) have recently undertaken a biochemical study of TLS at adducts of the HCA 2-amino-3-methylimidazo[4,5-f]quinoline (IQ) using purified human polymerases. In our current study of TLS, we describe our findings for adducts of PhIP, the most abundant HCA in cooked foods (4).

A rat colon cancer model induced by PhIP shows profiles of cancer development similar to the multistep model of colon carcinogenesis in humans (35). In this rat model, p53 and K-ras mutations are rarely observed, whereas mutations in *Apc* and its downstream gene β -catenin have been frequently observed (21, 36–38). Hence, mutations in *Apc* or β -catenin have been speculated to play a critical role in PhIP-induced colon carcinogenesis. Five mutations in the *Apc* gene were previously detected in four of eight PhIP-induced rat colon tumors, and all of these mutations involved a single guanine deletion in the 5'-GGGA-3' sequence (21). This characteristic mutation induced by PhIP, 5'-GGGA-3' to 5'-GGA-3', was also observed in other *in vivo* mutation analyses using transgenic animals harboring introduced reporter genes, such as *lacI* (18–20). Hence, the 5'-TCCGGGAAC-3' sequence corresponding to a mutation hot spot within the rat *Apc* gene, which we utilized to introduce the PhIP adduct and employed as the template for *in vitro* DNA synthesis analyses, could be a suitable model for revealing the molecular mechanisms associated with PhIP-induced mutations.

As discussed later, our results indicate a possible molecular mechanism for the 5'-GGGA-3' to 5'-GGA-3' mutation induced by PhIP.

DNA Polymerases Involved in TLS through the dG-PhIP Adduct—TLS through many DNA lesions requires the action of two different polymerases, an "inserter" and an "extender," the former to perform nucleotide insertions opposite the lesion site and the latter for subsequent extensions (39). The catalytic efficiency of the dCTP-insertion reaction opposite the dG-PhIP adduct by REV1 was found to be more than 2,000-fold greater than that by pol κ (see Tables 2 and 3). This result strongly suggests that REV1 functions *in vivo* as an inserter polymerase for TLS through the dG-PhIP adduct. This insertion step by REV1 is also error free. REV1 has been reported previously to insert dCTP opposite abasic sites and various N2-dG adducts (26, 39–41). However, our current study is the first to show that REV1 inserts dCTP opposite a large size C8-dG adduct. We used a shorter (C-terminal deleted) form of pol κ in our current experiments and an intact pol κ may be more effective for this insertion reaction. As for pol η , a detailed kinetic analysis was not performed. Hence, the possibility cannot be excluded that pol κ and pol η also function as inserter polymerases.

In addition to the Y-family DNA polymerases, DNA polymerase ζ (pol ζ), belonging to the B-family DNA polymerases, is considered to be involved in TLS through various lesions as an extender DNA polymerase (39, 42, 43). We have not carried out a primer extension assay with pol ζ and thus the possibility cannot be completely excluded by our current data that pol ζ functions *in vivo* as an extender polymerase for TLS through the dG-PhIP adduct. In our present study, we provide evidence that pol κ can extend from dC opposite the dG-C8-PhIP adduct *in vitro*. It is, therefore, possible that pol κ , at least partially, functions as an extender polymerase *in vivo* for TLS through the dG-PhIP adduct. Further study about cooperation between two or more DNA polymerases, including pol ζ , is necessary to verify which DNA polymerases are involved in the bypass synthesis through the PhIP lesion.

The catalytic efficiency of pol κ for a dGTP insertion into substrate C-p28 was a little higher than that for dCTP insertions (see Table 2 and Fig. 6D). The former generates a single guanine deletion, and the latter is an error-free extension. Consequently, our data suggest that the extension reaction with pol κ from the nucleotide opposite the dG-C8-PhIP adduct causes frequent single-guanine deletions from the GGG stretch. It has been reported that one characteristic feature of pol κ homologs, from bacteria to humans, is their propensity to generate single-base deletions (44–47). The crystal structure of Dpo4, a thermophilic archaea homolog of pol κ , in ternary complexes with DNA and an incoming nucleotide supports the model that a single base deletion by pol κ is generated through a misaligned intermediate complex where the template dG forms an extrahelical looped out structure and the incoming dGTP skips this extrahelical base and pairs with the next template base dC (48) (see supplemental Fig. S6). It is reasonable to speculate therefore that, in the case of TLS through dG-C8-PhIP, mammalian pol κ generates the single guanine deletion via a similar intermediate where the PhIP-adducted dG is looped out and template-primer slippage occurs. However, further analyses for

determining whether the one-base skipping of pol κ beyond the lesion observed by us is dependent on the nucleotide placed 5' to the lesion or not, are necessary to clarify the detailed molecular mechanism underlying one base skipping of pol κ .

Molecular Mechanisms Underlying Mutation Induction by PhIP—We have demonstrated herein by *in vitro* DNA synthesis analyses using oligonucleotide templates containing dG-PhIP that: 1) replicative DNA polymerases stall at the PhIP adduct and cannot perform translesional DNA synthesis beyond this point; 2) REV1 inserts a dC opposite the dG-PhIP with a much higher efficiency than other TLS polymerases, including pol κ and pol η ; and 3) pol κ has a potential ability to catalyze an extension reaction from the 5'-dC opposite the adduct and often skips over one dG in the template during this extension step. A working model for the induction of mutations at the PhIP adducts based on the results shown in the present study is illustrated in supplemental Fig. S6. This model could be adopted for other sequences containing a G repeat stretch longer than GGG.

REFERENCES

1. Nagao, M. (2000) in *Food Borne Carcinogens: Heterocyclic Amines* (Nagao, M., and Sugimura, T., eds) pp. 163–196, John Wiley & Sons Ltd., Chichester, UK
2. Schut, H. A., and Snyderwine, E. G. (1999) *Carcinogenesis* 20, 353–368
3. Felton, J. S., Knize, M. G., Shen, N. H., Lewis, P. R., Andresen, B. D., Happe, J., and Hatch, F. T. (1986) *Carcinogenesis* 7, 1081–1086
4. Felton, J. S., Jagerstad, M., Knize, M. G., Skog, K., and Wakabayashi, K. (2000) in *Food Borne Carcinogens: Heterocyclic Amines* (Nagao, M., and Sugimura, T., eds) pp. 31–71, John Wiley & Sons Ltd., Chichester, UK
5. Holme, J. A., Wallin, H., Brunborg, G., Söderlund, E. J., Hongso, J. K., and Alexander, J. (1989) *Carcinogenesis* 10, 1389–1396
6. Felton, J. S., and Knize, M. G. (1991) *Mutat. Res.* 259, 205–217
7. Ohgaki, H., Takayama, S., and Sugimura, T. (1991) *Mutat. Res.* 259, 399–410
8. Ito, N., Hasegawa, R., Sano, M., Tamano, S., Esumi, H., Takayama, S., and Sugimura, T. (1991) *Carcinogenesis* 12, 1503–1506
9. Sugimura, T., Wakabayashi, K., Nakagama, H., and Nagao, M. (2004) *Cancer Sci.* 95, 290–299
10. Imaida, K., Hagiwara, A., Yada, H., Masui, T., Hasegawa, R., Hirose, M., Sugimura, T., Ito, N., and Shirai, T. (1996) *Jpn. J. Cancer Res.* 87, 1116–1120
11. Frandsen, H., Grivas, S., Andersson, R., Dragsted, L., and Larsen, J. C. (1992) *Carcinogenesis* 13, 629–635
12. Lin, D., Kaderlik, K. R., Turesky, R. J., Miller, D. W., Lay, J. O., Jr., and Kadlubar, F. F. (1992) *Chem. Res. Toxicol.* 5, 691–697
13. Snyderwine, E. G., Davis, C. D., Nouso, K., Roller, P. P., and Schut, H. A. (1993) *Carcinogenesis* 14, 1389–1395
14. Schut, H. A., and Herzog, C. R. (1992) *Cancer Lett.* 67, 117–124
15. Endo, H., Schut, H. A., and Snyderwine, E. G. (1994) *Cancer Res.* 54, 3745–3751
16. Morgenthaler, P. M., and Holzhäuser, D. (1995) *Carcinogenesis* 16, 713–718
17. Yadollahi-Farsani, M., Gooderham, N. J., Davies, D. S., and Boobis, A. R. (1996) *Carcinogenesis* 17, 617–624
18. Okonogi, H., Stuart, G. R., Okochi, E., Ushijima, T., Sugimura, T., Glickman, B. W., and Nagao, M. (1997) *Mutat. Res.* 395, 93–99
19. Lynch, A. M., Gooderham, N. J., Davies, D. S., and Boobis, A. R. (1998) *Mutagenesis* 13, 601–605
20. Okochi, E., Watanabe, N., Shimada, Y., Takahashi, S., Wakazono, K., Shirai, T., Sugimura, T., Nagao, M., and Ushijima, T. (1999) *Carcinogenesis* 20, 1933–1988
21. Kakiuchi, H., Watanabe, M., Ushijima, T., Toyota, M., Imai, K., Weisburger, J. H., Sugimura, T., and Nagao, M. (1995) *Proc. Natl. Acad. Sci.*